Magnetic resonance imaging planning in children with complex congenital heart disease

Research Article

Journal of the Royal Society of Medicine Cardiovascular Disease
6 1–7

DOI: 10.1177/2048004017701870
journals.sagepub.com/home/cvd

Magnetic resonance imaging planning in children with complex congenital heart disease – A new approach

Israel Valverde[1], Tarinee Tangcharoen[2], Tarique Hussain[1,3], Hubrecht de Bliek[4], Graeme Penney[1], Marcel Breeuwer[4], Tobias Schaeffter[1], Reza Razavi[1] and Gerald Greil[1,3]

Abstract

Objectives: To compare a standard sequential *2D Planning Method* (2D-PM) with a *3D offline Planning Method* (3D-PM) based on 3D contrast-enhanced magnetic resonance angiography (CE-MRA) in children with congenital heart disease (CHD).

Design: In 14 children with complex CHD (mean: 2.6 years, range: 3 months to 7.6 years), axial and coronal cuts were obtained with single slice spin echo sequences to get the final double oblique longitudinal cut of the targeted anatomical structure (2D-PM, $n = 31$). On a separate workstation, similar maximal intensity projection (MIP) images were generated offline from a 3D CE-MRA. MIP images were localizers for repeated targeted imaging using the previous spin echo sequence (3D-PM). Finally, image coverage, spatial orientation and acquisition time were compared for 2D-PM and 3D-PM.

Main outcome measures: 2D-PM and 3D-PM images were similar: both perfectly covered the selected anatomic regions and no spatial differences were found ($p > 0.05$). The mean time for creation of the final imaging plane was 241 ± 31 s (2D-PM) compared to 71 ± 18 s (3D-PM) ($p < 0.05$).

Conclusions: 3D-PM shows similar results compared to 2D-PM, but allows faster and offline planning thereby reducing the scan time significantly. As newly developed high-resolution 3D datasets can also be used further improvement of this technology is expected.

Keywords

Cardiology, cardiovascular surgery, cardiovascular imaging agents/techniques, diagnostic testing, pediatric and congenital heart disease including cardiovascular surgery

Date received: 1 February 2017; accepted: 21 February 2017

Introduction

Cardiac magnetic resonance (CMR) is an ideal modality for the evaluation of children with congenital heart diseases (CHD). The first step in this CMR studies is usually the planning stage: its aim is to target the critical structures and acquire the best planes for its visualization, for further investigation using the most adequate CMR sequence. This is the most important preparatory step, and the success of the CMR study will highly depend on the accuracy of localizing and characterizing the anatomy of the primary and secondary lesions. It may be highly difficult and extremely time-consuming in children with complex CHD due to the small size of the cardiovascular structures and the complex spatial relationships of the different cardiac segments.[1]

[1]Division of Imaging Sciences and Biomedical Engineering, King s College London, London, UK
[2]Division of Cardiology, Department of Internal Medicine, Ramathibodi Hospital, Mahidol University, Bangkok, Thailand
[3]University of Texas Southwestern Medical Center at Dallas, Pediatric Cardiology, Children's Medical Center, Dallas, TX, USA
[4]Healthcare Informatics/Patient Monitoring, Philips Healthcare, Noord-Brabant, the Netherlands

Corresponding author:
Israel Valverde, Division of Imaging Sciences, St Thomas Hospital, King's College London, The Rayne Institute, 4th Floor, Lambeth Wing, London SE1 7EH, UK.
Email: isra.valverde@kcl.ac.uk

Dependent on institutional preferences and CMR system capabilities, different methods for image planning are used, such as real-time or interactive localizers.[2,3] However, they have one major limitation: the low spatial resolution. For this reason, in small children with complex CHD, a commonly used approach is an ECG-triggered high-resolution black-blood spin echo sequence to target these very small structures. To cover the full length of a vessel, two perpendicular cuts of this structure need to be acquired to position the final plane ideally in the center of the vessel lumen (Figure 1). Depending on the vessel size and the spatial orientation, several images may be necessary to image the vessel full length.

Therefore, an offline planning tool based on a commonly used 3D CMR sequence may be desirable in this group of patients. Scan time can be reduced with optimal slice position in small and unusual special oriented vascular structures. The purpose of this study was to compare the commonly used sequential planning method (2D-PM, Figure 1) with the new offline 3D planning tool (3D-PM, Figure 2) in children with complex CHD. Time efficiency differences in spatial orientation as well as intra- and inter-observer data between both methods were compared.

Methods

Institutional review board approval and informed consent were obtained for this prospective study. In 14 children (mean age: 2.6 years, range: 3 months–7.6 years, mean weight: 11.8 kg, range: 4.9–23.6 kg) with complex CHD, CMR was performed on a 1.5T system (Philips Healthcare, Best, The Netherlands). Patients were anesthetized according to our institutional protocol. Patients demographic characteristics are summarized in Table 1.

To compare this two planning approaches, the selected anatomical structures described in Table 1 were planned using (1) a commonly used sequential planning method (2D-PM, Figure 1) and (2) the newly introduced offline 3D planning technique (3D-PM, Figure 2). At the end of the CMR examination, 3D-PM was used as a localizer and the same black-blood sequence used for initial planning (2D-PM) was applied to image the structures based on 3D-PM.

2D-PM was based on an ECG-triggered high-resolution black-blood spin echo sequence (TR = 750 ms, TE = 30 ms, flip angle = 90 °, matrix = 512 × 512, FOV = 250–350 mm, slice thickness = 3–5 mm). Initially, a stack of 2D axial slices (Figure 1(a)) was acquired. A perpendicular cut through the selected vascular structure (e.g. right pulmonary artery, RPA) was then performed to obtain an oblique coronal plane (Figure 1(b)). Another plane through the selected structure in the previous coronal plane results in a double oblique plane ideally imaging the maximal length of the vessel (Figure 1(c)) or to demonstrate a stenosis in this vessel. After that, a three-dimensional contrast-enhanced magnetic resonance angiography (3D CE-MRA) was performed according to our standard institutional imaging protocol in these patients.

The proposed method 3D-PM (Figure 2) is based on the previous CE-MRA dataset (TR = 4.5 ms, TE = 1.5 ms, flip angle = 40 °, slice thickness = 0.6–2 mm, matrix = 512 × 240). Contrast agent (0.1 mmol/kg; Magnevist, Berlex Laboratories, New Jersey, USA) was manually injected and two sequential 3D CE-MRA acquisitions of 10 to 12 s each were performed during a single breath-hold in an anesthetized patient. The 3D CE-MRA dataset was sent for post-processing to a separate workstation (ViewForum, Philips Healthcare, The Netherlands). The desired imaging planes were reformatted offline as maximal

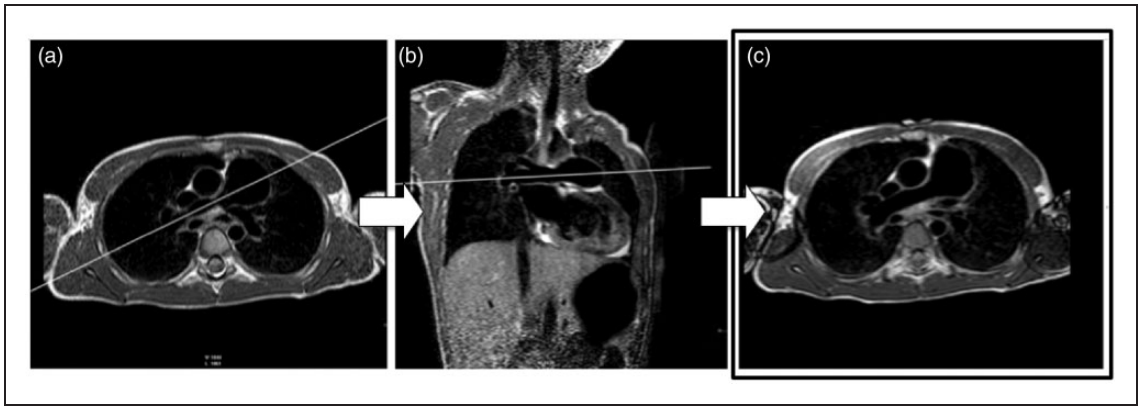

Figure 1. Method 1 (2D-PM) used sequential axial black-blood spin echo sequences (a to c) to create a long axis cut in the center of the right pulmonary artery to demonstrate its full length. (a) From a stack of axial planes, the center of the right pulmonary artery is cut (a, white line) resulting in an oblique-coronal plane (b). Using image plane a and b as a reference a double-oblique plane (c) demonstrate the full length of the right pulmonary artery.

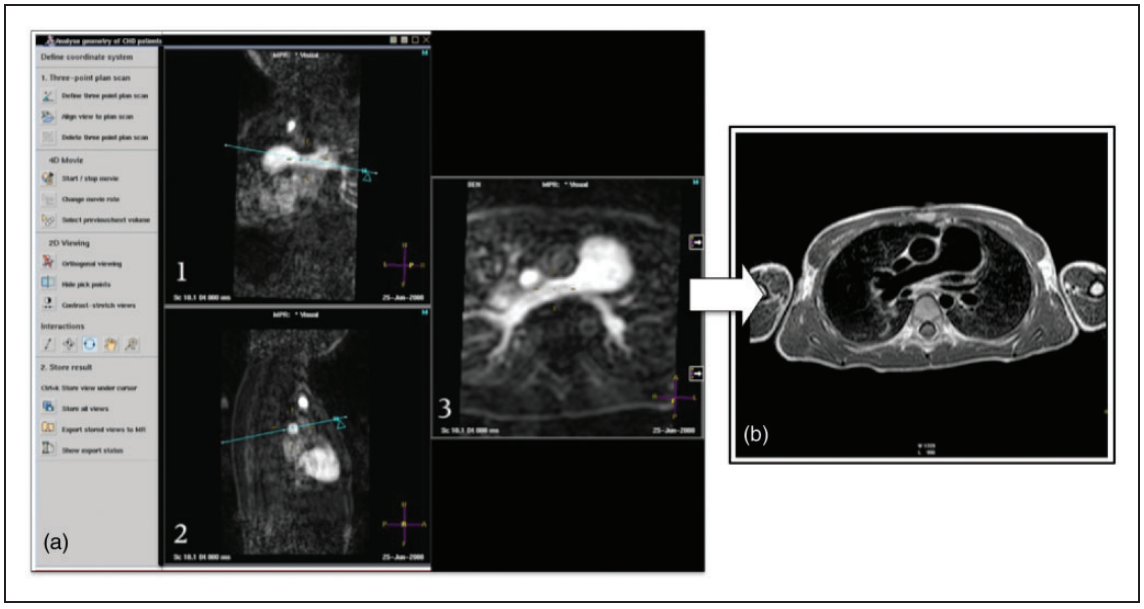

Figure 2. Method 2 (3D-PM) allows offline planning of a similar oblique axial cut of the right pulmonary artery (b corresponds to Figure 1(c)) based on a previously acquired 3D contrast-enhanced magnetic resonance angiography (3D CE-MRA) dataset (a). Using different viewports (a1: oblique-coronal; a2: oblique-sagittal; a3: final double oblique axial plane covering the maximal length of the RPA). The plane coordinates of a3 are transmitted to the CMR console to acquire the black-blood spin echo for comparison with Figure 1(c). As b is acquired after contrast agent administration, vessel walls show bright signal due to enhancement. Image quality was sufficient to compare Figures 1(c) and 2(b) qualitatively and quantitatively.

intensity projection (MIP) images on the workstation (Figure 2). During this time, the CMR console was free to run other sequences. Reformatted MIP images were retransferred to the CMR console and its spatial coordinates were used to plan another black-blood spin echo image. Black-blood images of 2D-PM and 3D-PM of the selected anatomic structure (Table 1) were evaluated using the following criteria.

Coverage of the anatomic regions

Acquired black-blood images were visually examined by two experienced pediatric cardiologists (IV with 3 years and GFG with more than 10 years experience in cardiac CMR). Images were presented in a random order. Image quality was assessed regarding the identification and coverage of the selected structure[4]: Grade 1 (targeted structure optimal imaged): no visible difference noticed between images created by 2D-PM and 3D-PM, Grade 2 (targeted structure well imaged): both images of diagnostic quality but slightly visible differences noticed between image created by 2D-PM and 3D-PM, Grade 3 (targeted structure imaged differently): visible coverage differences noticed between images created by 2D-PM and 3D-PM. The second set of black-blood images was acquired after the administration of contrast agent using method 3D-PM. This resulted in contrast enhancement of the vessel wall but anatomical structures were easily comparable (Figures 1 and 2).

Quantitative evaluation of spatial coordinates

Quantitative differences between the spatial coordinates of the acquired imaging planes were analyzed. The centre of the planes obtained using 2D-PM (Figure 1(c)) and 3D-PM (Figure 2(b)) was determined. The mean perpendicular distance, calculated in the centre of both planes, was used to determine the distance between them. The orientation of each plane referred to the standard orthogonal planes (axial, coronal and sagittal) was also determined to assess the differences between the two methods.

Time evaluation

2D-PM time was measured from the beginning of the planning procedure to the start of the final black-blood sequence. 3D-PM time started as soon as the CE-MRA dataset was available for reformatting until the black-blood sequence for final image data acquisition was started. The number of cases was recorded until the investigators felt familiar with this software were recorded. Finally, comparison of the time required obtaining the final planes between 2D-PM and 3D-PM was calculated.

Table 1. Patients' characteristics.

Patient	Age (years) (2.6 ± 2.8)	Weight (kg) (11.8 ± 6.6)	Height (cm) (83.1 ± 22)	BSA (3D-PM) (0.5 ± 0.2)	Cardiac diagnosis	Previous interventions	CMR planes
1	0.7	6.0	60	0.32	Coarctation of the aorta	Balloon angioplasty	Aortic arch sagittal
2	5.8	11.3	90	0.53	DORV	BT shunt	LVOT sagittal LVOT coronal
3	0.4	14.9	93	0.62	Double aortic arch	Surgical division anterior arch	LPA sagittal LPA axial RPA coronal RPA axial
4	1.2	7.8	76	0.41	PA, VSD	BT shunt	LPA axial RPA axial
5	0.8	6.6	68	0.35	Tricuspid atresia	BT shunt	RPA coronal RPA axial LVOT sagittal LVOT coronal
6	6.9	20.0	113	0.79	Coarctation of the aorta	Balloon angioplasty	Aortic arch sagittal Four chamber view
7	2.1	11.3	81	0.50	HLHS	Norwood stage I and II	LPA sagittal LPA axial
8	0.3	4.9	56	0.28	HLHS	Norwood stage I	LPA sagittal LPA axial Aortic arch sagittal
9	2.8	18.1	96	0.70	PA, IVS (TOF type)	PDA stent	LPA axial RPA axial
10	1.2	7.5	73	0.39	HLHS	BT shunt	RPA coronal RPA axial
11	7.7	21.8	121	0.85	TOF	RVOT patch	RPA axial LPA axial
12	0.7	6.3	64	0.33	PA, VSD (TOF type)	BT shunt	RPA axial
13	0.4	5.2	58	0.29	HLHS	Norwood stage I and II	RPA axial LPA axial
14	6.3	23.6	115	0.87	HLHS	Norwood stage I and II, Fontan	LPA sagittal LPA axial

Note: values are expressed as median $\pm$ SD.

BTS: Blalock-Taussig shunt; DORV: double outlet right ventricle; HLHS: hypoplastic left heart syndrome; IVS: intact ventricular septum; LPA: left pulmonary artery; LVOT: left ventricular outflow tract; PA: pulmonary atresia; PDA: persistent ductus arteriosus; RPA: right pulmonary artery; RVOT: right ventricular outflow tract; TOF: Tetralogy of Fallot; VSD: ventricular septal defect.

Statistical analysis

Results are expressed as means $\pm$ 1 standard deviation for normally distributed data. Friedman's test was used to evaluate the difference in image quality score. The agreement between the distance and angulations between the two methods was evaluated by a paired t-test and plotted in the Bland-Altman graphs. Required time to perform 3D-PM was assessed by the inter-observer variability. Difference of time required for 2D-PM and 3D-PM was determined using an independent t-test. Analysis was performed by using statistical software (SPSS, version 17; SPSS, Chicago, IL). A p value of less than 0.05 was considered to indicate a statistically significant difference.

Results

Coverage of the anatomic regions

Two investigators compared the anatomic coverage of both methods based on a previously described qualitative scale. No visible differences in the anatomic coverage between 2D-PM and 3D-PM (Grade 1) were found

in 26 cases. Slightly visible differences, but with diagnostic quality (Grade 2), were found in three cases. No severe differences (Grade 3) were found in any of the cases. Summarizing, no coverage of statistically significant differences was found between 2D-PM and 3D-PM ($p > 0.05$).

Quantitative evaluation of spatial coordinates

The absolute mean distance between the centers of the planes was 1.8 mm (SD ± 2 mm, range 0.1 to 8.9 mm). The angular mean differences and standard deviation were 1.3 ± 6.3 degrees in the axial plane, 2.6 ± 7.9 degrees in the coronal plane and 0.7 ± 6.5 degrees in the sagittal plane. A paired t-test showed no statistically significant difference in the plane orientation for axial ($p = 0.275$), for coronal ($p = 0.074$) or for sagittal planes (0.559). The values are plotted in Figure 4 and summarized in Table 2.

Time evaluation

Two experienced cardiologists used the new software (3D-PM). Three training cases were given to both cardiologists to get used to the new software. Images planes were reformatted in a mean time of 69 s and 74 s. No significant differences were found between the two investigators (3D-PM method, paired t-test $p = 0.23$). On the other hand, the mean time to obtain the desired plane using 2D-PM was 241 ± 31 s. 2D-PM was statistically significantly slower than 3D-PM (independent t-test, $p < 0.001$).

Discussion

Current CMR planning of CHD requires time-efficient and flexible methods, as scanner time is expensive, cardiac and vascular anatomy is complex and sedation or general anesthesia time should be as short as possible. Although there are different planning strategies depending on the institution or vendor preferences (i.e. real-time interactive steady-state free precession, single-shot techniques like Half Fourier Acquisition Single shot Turbo spin Echo *HASTE* etc.), all of them need a skilled investigator at the scanner console. The purpose of this study was to find an accurate and fast alternative planning method for complex CHD in small children. To achieve this, a 3D CE-MRA of the chest with sufficient resolution according to patient size allowed MIP reformats of any vascular structure, even when small and intricate. This 3D CE-MRA was part of the standard imaging protocol in this patient group and was not intended to be used for image slice planning. User friendly and intuitive software allowed time-efficient reformatting of the desired anatomical structure and transfer of the MIP image to the scanner console for further sequence planning. As this software was running on a separate workstation, scanner time was available to run and plan additional sequences on the scanner console.

The proposed 3D-PM accurately located the selected anatomic structures compared with the traditional method 2D-PM. The absolute mean distance found between the centre of the planes was 1.8 ± 2.0 mm and the distance between planes showed a good correlation between both methods independently of the body surface area (Figure 4, $R^2 = 0.008$). When comparing the angular differences in the axial, coronal and sagittal planes between the two methods, no statistically significant differences (paired t-test, $p > 0.05$) and a good agreement were found (Figure 4). Differences were further reduced when planning small structures such as pulmonary arteries. For example, the mean difference and standard deviation for the LPA were 1.1 ± 0.8 mm and for the RPA were 1.2 ± 0.7 mm. This shows that the tool is accurate enough for planning small vascular structures (e.g. branch pulmonary arteries in small children). Differences may be much more related to inter-observer variability as it may be difficult for two observers to chose the same center in a large vessels such as the aorta (Figure 3, *) or the four-chamber view of the heart (Figure 3, §). However, although both planes (2D-PM and 3D-PM) were different in

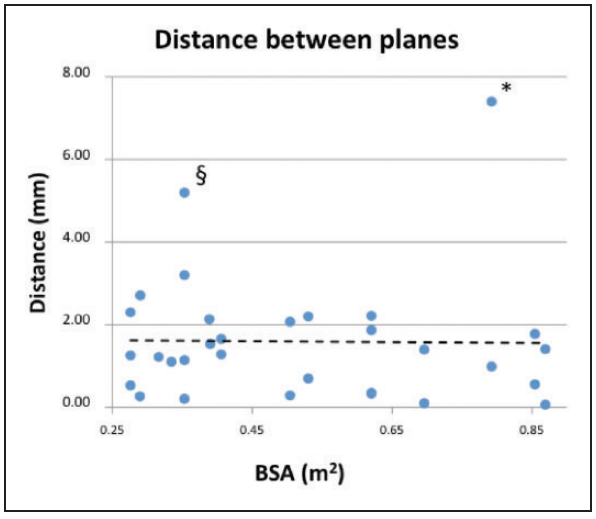

Figure 3. The scatter chart shows the distance between the planes created by 2D-PM (Figure 1) and 3D-PM (Figure 2). The X-axis represents the body surface area (BSA) in 3D-PM and the Y-axis represents the mean absolute distance in mm between the centers of the two planes (e.g. image Figure 1(c) and 2(b)). Outliers (§ = four-chamber view of the heart and * = aorta inplane) are explained by different targeted anatomic structures (see also text).

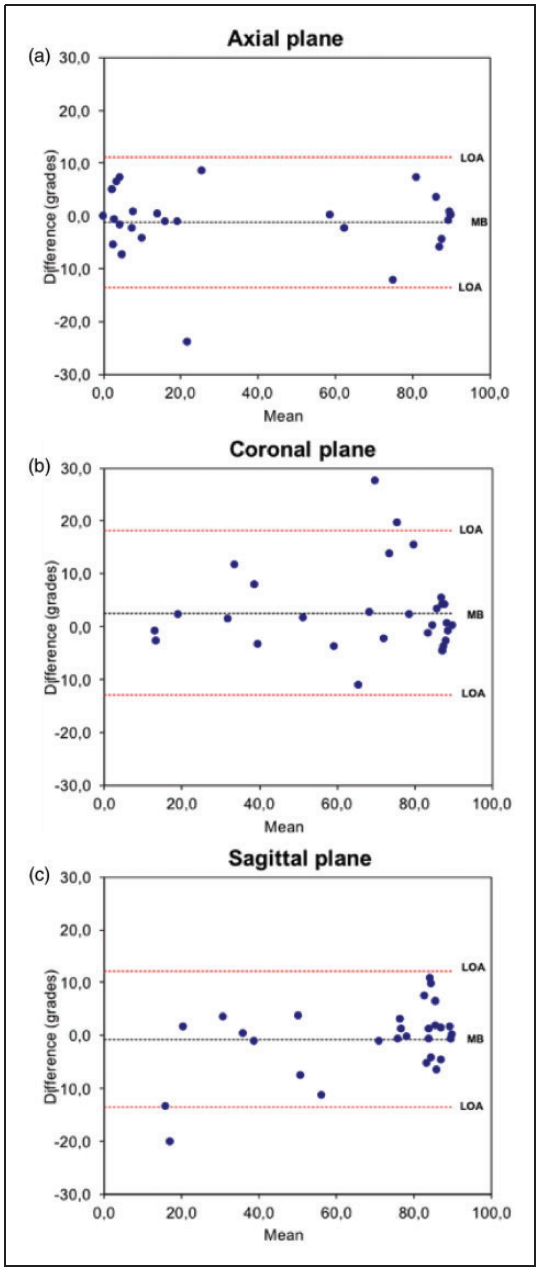

Figure 4. Bland-Altman plots of the mean bias (MB) for the angular differences (degrees) in the axial (a), coronal (b) and sagittal (c) planes between the planes obtained with the currently used sequential black blood method (2D-PM, Figure 1(c)) and the new offline method (3D-PM, Figure 1(b)); 95% confidence limits of agreement (LOA). Outliers are explained by different targeted structures (see also text).

angulations, they perfectly covered the anatomic structures with no differences as judged by the two observers.

Maximum angular differences were found in the pulmonary artery planes. The outliers (Figure 4) were explained retrospectively because the two observers have chosen different side branches of the right or left pulmonary arteries. However, the main pulmonary arteries were successfully imaged by both observers. Also the differences in the planning of a sagittal cut in a tortuous aortic arch in a 4.9 kg infant with hypoplastic left heart syndrome and aortic atresia (after a Norwood I procedure) is referred to slightly different planning of the vessel center. If these cases were excluded, excellent results were achieved. This shows the ability of this tool to plan very accurately the desired imaging plane particularly in small children with CHD and small vascular structures.

Regarding the scan time, the inter-observer planning time variability using the new tool was not statistically significant between the two observers after a short introduction of three cases (t-test, $p = 0.23$). This demonstrates the practical use of this method as it is easy to learn for any experienced investigator. Furthermore, 3D-PM proved to be much more time efficient than 2D-PM (2D-PM 241 ± 31 s compared to 3D-PM 71 ± 18 s, $p<0.001$). This is particularly important as patients are under GA or sedated and scanner time is very expensive. Furthermore, using teleradiology one experienced pediatric cardiologist or radiologist can plan complex cuts in different patients, while the actual scans are run by different radiographers. It is very likely that 3D-PM may also benefit from the constantly improving image quality of 3D CMR datasets. Respiratory navigator gated and ECG-triggered 3D steady-state-free precession (3D SSFP) techniques provide already excellent image quality of the heart and part of the great vessels in young patients and adults with CHD.

The limitations in applicability in a single center and limited number of patients study must be acknowledged. Although in the current study CE-MRA was used, not all CHD patients require administration of contrast agents. Future studies might be based on respiratory navigator gated and ECG-triggered 3D-SSFP datasets. As no contrast agent is required, this technique could also be used in patients with renal failure.

In summary, the new proposed 3D-PM allows time efficient and precise slice selection of complex vascular structures in small children with CHD. Reformatting the CMR images in a separate workstation opens the door for the future use of teleradiology using 3D-PM, which may allow an experienced investigator to run several pediatric cardiology examinations in parallel or to support colleagues during the CMR scan at remote sites. Future studies might be based on respiratory navigator gated and ECG-triggered 3D-SSFP datasets.

Table 2. The commonly used sequential imaging method (2D-PM, Figure 1) and offline CE-MRA method (3D-PM, Figure 2) were compared (see Table 1, 31 planes analyzed).

	2D-PM	3D-PM	Differences
Quantitative evaluation of the spatial coordinates			
Distance between the centre of the planes (mm)			1.8 ± 2.0
Angulations of the planes (degrees)			
Axial	39.1 ± 38.4	40.4 ± 38.4	1.3 ± 6.3 ($p = 0.275$)
Coronal	69.4 ± 25.2	66.8 ± 25.2	-2.6 ± 7.9 ($p = 0.074$)
Sagittal	69.3 ± 25.8	70.0 ± 22.8	0.7 ± 6.5 ($p = 0.559$)
Evaluation of the time			
Time required to obtain the final plane (s)	241 ± 31	71 ± 18	170 ± 18.3 ($p < 0.001$)

Note: Values are expressed as mean $\pm$ SD.

Contributorship

All authors were involved in the design phase, the analysis and the interpretation of the results. IV and GG drafted the manuscript, and all authors approved the final version.

Declaration of conflicting interests

The author(s) declared no potential conflicts of interest with respect to the research, authorship, and/or publication of this article. MB and HB work for Philips Healthcare.

Funding

The author(s) disclosed receipt of the following financial support for the research, authorship, and/or publication of this article: This work was supported by the Talentia Excellence Grant (awarded by the Ministry for Innovation, Science and Enterprise, Andalusia, Spain) and the Advanced Research Fellowship Grant (awarded by the Engineering and Physical Sciences Research Council, UK, GR/T02799/03).

Ethical approval

Institutional review board approval and informed consent were obtained for this prospective study.

Guarantor

IV.

References

1. Anderson RH, Razavi R and Taylor AM. Cardiac anatomy revisited. *J Anat* 2004; 205: 159–177.
2. Lee VS, Resnick D, Bundy JM, et al. Cardiac function: MR evaluation in one breath hold with real-time true fast imaging with steady-state precession. *Radiology* 2002; 222: 835–842.
3. Taylor AM and Bogaert J. Cardiovascular MR imaging planes and segmentation. *Clin Cardiac MRI* 2012; 2: 93–107.
4. Bossuyt PM, Reitsma JB, Bruns DE, et al. Towards complete and accurate reporting of studies of diagnostic accuracy: the STARD initiative. *Vet Clin Pathol* 2007; 36: 8–12.